Properties of New Magnetic Surfactants

Paul Brown[a], Alexey Bushmelev[b], Craig P. Butts[a], Jean-Charles Eloi[c], Isabelle Grillo[d], Peter J. Baker[e], Annette M. Schmidt[b] and Julian Eastoe*[,a]

[a]*School of Chemistry, University of Bristol, Cantock's Close, Bristol BS8 1TS, U.K.;* [b]*Department Chemie, Universität zu Köln, Luxemberger Strasse 116, 50939 Köln, Germany;* [c]*H. H. Wills Physics Laboratory, University of Bristol, Tyndall Avenue, Bristol BS8 1TS, U.K.;* [d]*Institut Max-von-Laue-Paul-Langevin, BP 156-X, F-38042 Grenoble Cedex, France;* [e]*ISIS-STFC, Rutherford Appleton Laboratory, Chilton, Oxon OX11 0QX, U.K.*

Graphical Abstract

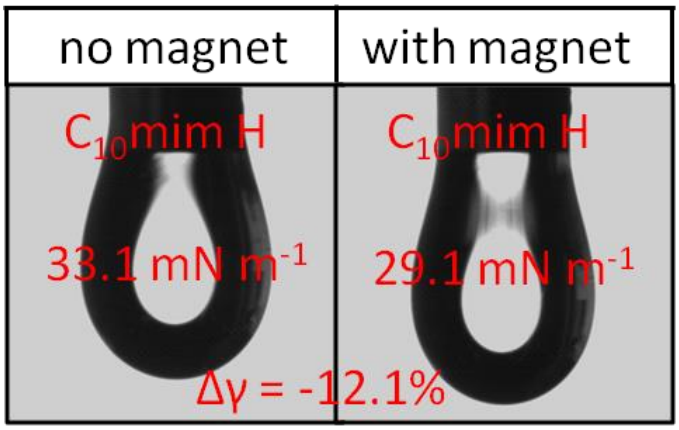

Abstract

This paper describes the synthesis and detailed characterization of a new set of magnetic surfactants containing lanthanide metal counterions. SQUID magnetometry has been used to elucidate the magnetic phase behaviour, and small-angle neutron scattering (SANS) provides evidence of micellar aggregation in aqueous media. This study also reveals that for cationic surfactants in aqueous systems there appears to be no significant increase in magnetic susceptibility after micellization.

Key Words

Magnetic surfactants, lanthanide based surfactants, SQUID magnetometry

Introduction

Recently, a new class of surfactants has been discovered which respond to a magnetic field.[1] These magneto-responsive surfactants are based on common cationic surfactants with metal complex anions, which, because they contain high effective concentrations of metal centres, allow physico-chemical properties to be controlled non-invasively and reversibly by external magnetic fields.

Surprisingly, even dilute micellar solutions of these paramagnetic surfactants exhibit a magnetic response, opening up new possibilities for control over interfaces, dispersions, colloids and nano-particles. It has been shown that magnetic emulsions can be readily generated from lubrication oil and brine, with suggested applications ranging from environmental cleanup, water treatment, separation and enhanced oil recovery.[2] They also show potential for use in catalysis, microfluidics and targeted drug delivery. It has been demonstrated that the controlled conjugation of magnetic surfactants to DNA (and other biomolecules) is possible allowing for manipulation in solution simply by switching “on” and “off” a magnetic field.[3]

This work increases the number of known magneto-surfactants by introducing new *f*-block metal based compounds, using SQUID magnetometry to provide a detailed investigation into magnetic properties. Here, this new work establishes the generality of the concept of magnetic surfactants. The use of *f*-block metals (transition metals having populated *f*-orbitals) is important not only because they have the highest known effective magnetic moments, but because they also have interesting magnetic phase behaviour, exhibiting ferro- or antiferromagnetism as well as paramagnetism. Lanthanide metals also have uses as catalysts,[4] superconductors,[5] active ions in luminescent materials used in optoelectronics and ceramics,[6] and as surfactant counterions they have been used in spectroscopic studies because of their well defined luminescence.[7]

It is important to note that the structures of the magnetic materials presented in this paper include no covalent bonds between spin sites. As such, they may be considered as a novel and interesting variant of molecular magnets, whereby the organic surfactant moiety provides some control over magnetic behaviour through partitioning of the metal ions.[8] As the organic moiety is also surface

active it is interesting to investigate whether self-aggregation might lead to further control of magnetic behaviour.

It has recently been shown that magnetic water-in-oil microemulsions can be made using magnetic anionic surfactants (based on transition and lanthanide metals). These magneto-responsive microemulsions exhibit superparamagnetism and unprecedented magnetic susceptibilities owing to a lack of bulk anisotropy due to the partitioning of surfactant molecules at the water/oil interface.[9] This paper furthers the field by investigating the susceptibility of micellar solutions in order to elucidate whether the formation of micelles at the critical micelle concentration (cmc) gives rise to any additional magnetic effects.

Experimental

Materials and Synthesis

1-decyl-3-methyl imidazolium chloride ([C_{10}mimCl, 96 %), dodecyltrimethylammonium bromide (DTAB, ≥ 98%), gadolinium chloride hexahydrate (99 %), holmium chloride hexahydrate (99.9%) and cerium chloride heptahydrate (99.9 %), were purchased from Sigma Aldrich and used without further purification. All compounds were synthesized according to previously reported literature,[10] whereby 1 eq. of metal trichloride was added to a methanolic solution of 1 eq. of either DTAB or C_{10}mim Cl and stirred overnight at room temperature, then dehydrated *in vacuo* at 80 °C overnight.

Polarizing Light Microscopy (PLM)

A Nikon Optiphot-2 microscope fitted with polarizing filters was used, and images were captured on a PC via a video camera and colour processor connected to the microscope. The liquid crystal phase progression of each surfactant was investigated by the solvent penetration method (i.e. phase cut).[11]

Electrical Conductivity Measurements

Electrical conductivities, κ, were determined using a Jenway Model 4510 Conductivity/TDS conductivity meter with temperature controlled at (25 ± 0.1) ˚C (thermostatic water bath). Critical micelle concentrations (cmc) were determined as normal, from the break points between the high {dκ/d(conc)} and low {dκ/d(conc)} branches of behaviour. Surfactant ionic dissociation constants (β), were estimated using the ratio of the slopes method.[12]

Small-Angle Neutron Scattering (SANS)

Scattering was measured on the D22 diffractometer at ILL, Grenoble, France. D22 is a reactor-based diffractometer, and a neutron wavelength of λ = 10 Å was employed at two different detector distances giving $0.0024 < Q < 0.37$ Å^{-1}. Appropriate normalization using site-specific procedures gave the absolute cross section I(Q) (cm^{-1}) as a function of momentum transfer Q (Å^{-1}). Measurements of the dilute aqueous systems were carried out in D_2O (scattering length density ρ = 6.33 x 10^{10} cm^{-2}) to provide the necessary contrast, and were placed in Hellma fused silica cuvettes with a path length of 2 mm. Raw SANS data was normalized by subtracting the scattering of the empty cell and a solvent background, using appropriate transmission measurements. Any low level of residual incoherent scattering was accounted for by a flat background term during the fitting process. Details on data analysis, and scattering laws employed in the model fitting, are presented in *Supporting Information*.

SQUID Magnetometry

Magnetic susceptibility data were collected for dried surfactant samples, placed in sealed polypropylene tubes and mounted inside a plastic straw for measurements in a magnetometer equipped with a superconducting quantum interference device (SQUID, MPMS XL-5, Quantum Design, San Diego, USA) and reciprocating sample option (RSO). After demagnetizing at 298K, the samples were cooled in zero field to 5 K. The data were then collected in 500 Oe from 5 to 300K at 2 K min^{-1}. Low temperature measurements of C10mimH were repeated on a SQUID MPMS XL-7 instrument (Quantum Design, San Diego, USA).

Surface Tensiometry

Surface tensions between aqueous surfactant solutions and air were performed at (25 ± 1) °C using a Krüss Drop Shape Analysis DSA1 apparatus. This instrument obtains spatial coordinates of a drop edge (shape and size), which are used to calculate surface tension[13]. Prior to use, the capillary needle (diameter 1.834 mm) and syringe were rinsed with copious amounts of pure water. Before being mounted on the dosing dispenser, the syringe was rinsed a few times with the surfactant solution to be measured. An aqueous drop was manually formed at the tip of the capillary. Measurements were acquired until steady values of surface tension were reached. Calibration used the surface tension of pure water (Elga, 18 MΩ cm).[14]

Measurements of surfactant aqueous solutions at 0.10 M were taken on the same drop with and without a magnet: NdFeB (N42, 20 mm x 10 mm magnetic field density of 0.44 T on the surface and a gradient of about 36 mT mm^{-2}) and was held in position at an approximate distance of 1 mm from the bottom of the drop surface.

Vibrating Sample Magnetometry

Quasi-static magnetometry is performed on an ADE Magnetics Vibrating Sample Magnetometer (VSM) EV7. The magnetization curves are monitored at 298 K and 75 Hz head drive frequency on samples sealed in Teflon vessels and placed on a glass sample holder between two poles of an electromagnet allowing a field range of -2.2 T – 2.2 T. All samples were measured in sealed Teflon pots. The raw data were corrected by subtraction of the signal of an empty pot. All curves were fitted as straight lines, and the volume susceptibility was calculated from the gradient of the slope. The diamagnetic susceptibility of water was also subtracted to calculate the susceptibility of paramagnetic material. From this the molar susceptibilities and magnetic effective moment were calculated. Samples with surfactant concentrations from 25 mM to 200 mM were measured three times, whereas samples with a surfactant concentration of from 2.5 mM to 20 mM were measured five times.

Results and Discussion

The synthesis of these new magnetic surfactants (Figure 1, note DTAG and DTAH have been reported previously[3]) is facile and may be applied to most commercially available cationic surfactants. The choice of cationic surfactant is practically unlimited offering new possibilities for molecular design of specialist surfactants.

Name	Anion	Cation
DTAB DTAG DTAH DTAC	Br^- $[GdCl_3Br]^-$ $[HoCl_3Br]^-$ $[CeCl_3Br]^-$	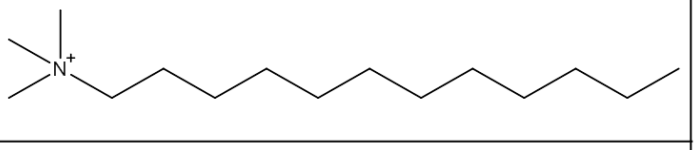
C_{10}mim Cl C_{10}mim G C_{10}mim H C_{10}mim C	Cl^- $[GdCl_4]^-$ $[HoCl_4]^-$ $[CeCl_4]^-$	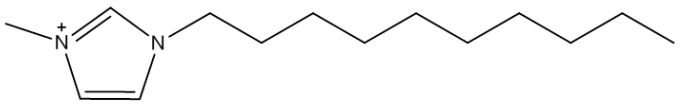

Figure 1: Compounds studied (DTAB and [C_{10}mim]Cl are non-magnetic).

Phase Behaviour – PLM

Polarizing light microscopy (PLM) textures (Figure 2) show that all the compounds exhibit some transition from fluid micellar to liquid crystalline phases, understood as arising from a competition between the increase in free energy associated with loss of orientational entropy against excluded volume and other interactions. The phase progression of the non-magnetic parent surfactants DTAB and C_{10}mimCl at 25˚C are consistent with literature: DTAB L_1-H_α–crystals[15] (where L_1 represents a non-birefringent micellar solution, H_α the mosaic texture of a reverse hexagonal phase); and [C_{10}mim]Cl exhibits a fan-like texture characteristic of a hexagonal phase (or focal conic lamellar phase).[1] Mesophase formation changes on progression to the magnetic analogues, with dilute lamellar phases appearing. Interestingly, mesophases did not form with the previously reported Fe(III)-based surfactants,[1] but they are observed here due to the increased hydrophilicity and large hydration numbers (typically around 5-6 for iron (III) and 8-9 for trivalent lanthanide metals) of the metal counterions.

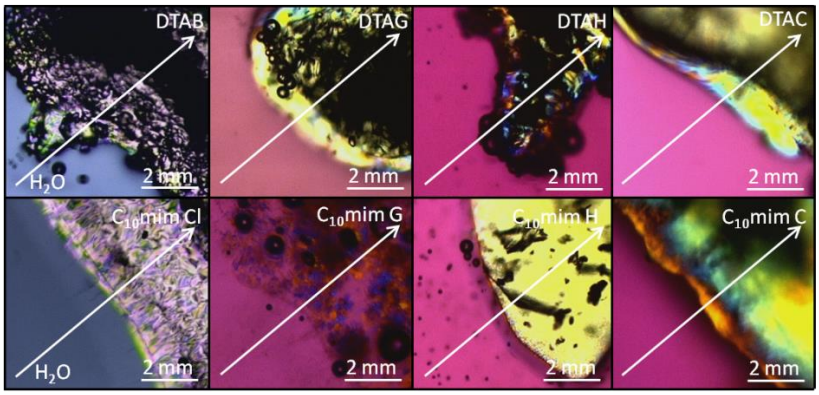

Figure 2: PLM textures showing mesophase formation of surfactants studied on addition of water at 25 ˚C.

CMC Determination by Electrical Conductivity

Electrical conductivity measurements of dilute aqueous solutions show that the critical micelle concentrations (cmcs, Table 2) are reduced by exchanging halides with lanthanide containing anions. However, values of the dissociation constant, β, suggest that the degree of counterion binding is low. This is also surprising as the large *f*-block anions should be less effective at screening cation-cation headgroup repulsions, thus increasing the cmc. A similar result was recently reported for iron based surfactants, and was explained in terms of counterion partitioning into the micellar core.[1] However, for more hydrophilic counterions this may, in part, be a result of partial coordination of the cation-anion pair.

Micellar Structure by SANS

Small-angle neutron scattering (SANS) shows unambiguously that these surfactants aggregate above the cmc. Data were collected (Figure 3, Table 1) for every compound except Gd-based surfactants (owing to the high neutron absorbance). At 0.04 M the inert parent surfactant DTAB formed ellipsoidal aggregates of radius 18 Å and aspect ratio, X = 1.4, commensurate with the alkyl chain length and agreeing with literature[16]. On exchanging the counterion almost no change in shape or size was observed and importantly almost all structure factor ((SQ)), which represents interparticle interactions between micelles, was lost.

Similar observations were seen for the imidazolium based surfactants (Figure 3, Table 1). However, the Ce- and Ho-based surfactants lead to some larger scale aggregates, indicated by enhanced scattering at low Q, and were fitted using an ellipsoid model rather than the spherical model used for the chloride analogue.

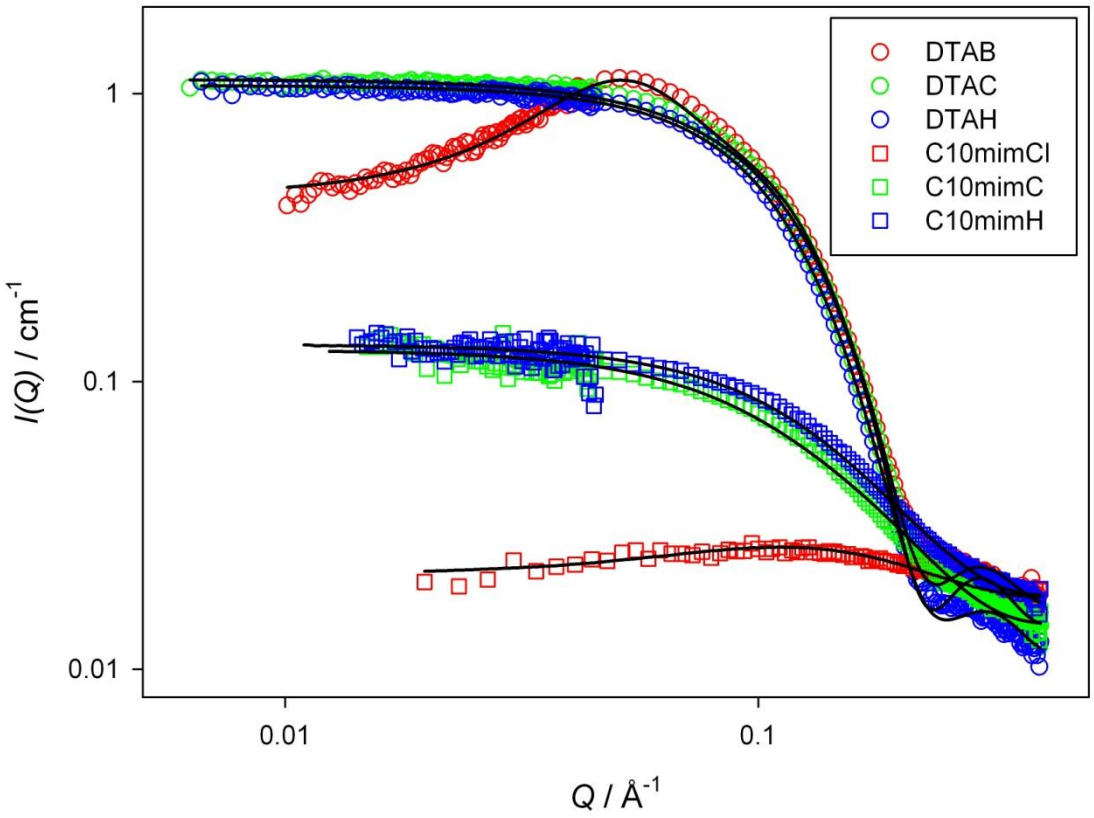

Figure 3 : SANS profiles for inert and magnetic surfactants. Lines through data are fits using models for charged ellipsoid micelles or non-interacting spherical micelles (*Supporting Information),* with parameters listed in Table 1. C_{10}mimCl 0.04 M (□), C_{10}mimCl 0.04 M (□), C_{10}mimCl 0.04 M (□), DTAB 0.04 M (o),DTAC 0.04 M (o),DTAH 0.04 M (o).

Compound	R_1 / Å ± 1	X ± 0.2
DTAB	18.0 (19.8)[16]	1.4 (1.2)[16]
DTAC	18.0	1.3
DTAH	17.4	1.6
C10mim Cl	11.0 (10.0)[17, a]	1.0 (1.0)[17, a]
C10mim C	10.1	3.3
C10mim H	10.4	2.4

Table 1: Parameters fitted to SANS data using the Hayter-Penfold model for ellipsoid micelles with a hard sphere structure factor (HSSQ). Brackets indicate literature values.

[a]Data recorded at 0.05 M.

Magnetic Properties of Bulk Surfactants

All the compounds displayed simple paramagnetic behaviour at room temperature. DTAH had the highest $\chi_m T$ value of all the surfactants (10.15 emu K mol^{-1} Oe^{-1}) corresponding to an effective paramagnetic moment of 9.05 μ_B (Table 2), followed by C_{10}mimH (8.55 emu K mol^{-1} Oe^{-1}, 8.30 μ_B). These values are lower than the theoretical spin-only values (Ho^{3+} has the $^5I_8$ electronic ground state, with the predicted effective magnetic moment, g[J(J+1)]$^{1/2}$ giving 10.61 μ_B).

The same pattern was observed for Gd and Ce based surfactants with tetraalkylammonium analogues exhibiting effective magnetic moments above the respective imidazolium analogues. It is especially surprising to see such a change in effective magnetic moment on exchanging the surfactant tail-group, since lanthanide metals possess 4f (inner) electrons that are effectively shielded from the influence of external forces by the overlying $5s^2$ and $5p^6$ shells. Therefore, they have large spin-orbit couplings resulting in large effective magnetic moments, but only weak ligand field effects. Based on molecular packing arguments, we may speculate that the DTAB analogues are less amorphous than the imidazolium based surfactants, resulting in stronger long-range structural ordering, long-range interactions, and thus a certain coupling effect between the metallic centers.

From SQUID magnetometry data (Figure 4) it is clear that most of the compounds exhibit magnetic phase transitions. Firstly, for DTAH a reduction of effective magnetic moment ($\chi_m T$) is observed on decreasing temperature, resulting in a Curie temperature (T_c) at 5.1 K. Only weak

ferromagnetic interactions are observed as seen by the positive Curie-Weiss values (Table 1) value, θ_{cw} = 4.09 K. A Néel temperature, T_N, around 133 K occurs in crystalline Ho[18] but no such transition was observed within the studied range. C_{10}mimH exhibits much the same behaviour as DTAH (Figure 4, S1 and S2), however a T_c was not observed above 5 K as indicated by a plot of $1/\chi_m$ as a function of temperature (Figure S2 and S3), which is linear. Unlike for DTAH, without any obvious magnetic transition the calculated value of θ_{cw} = 2.78 K for C_{10}mimH gives an approximate upper bound on the possible ordering temperature. A full hysteresis slope of the solid sample at 2 K (Figure S4) supports this conclusion as no hysteresis was observed. In addition, the curve can be distributed into two components by fitting with the Langevin function, one having a magnetic moment of 4.6 μ_B and the other 2.7 μ_B, both of which are too small to suggest a ferromagnetic state.

The gadolinium compounds showed no sign of a Néel temperature, T_N, (which occurs at 298.4 K in the pure metal[19]) and followed the Curie-Weiss law within the measured regime.

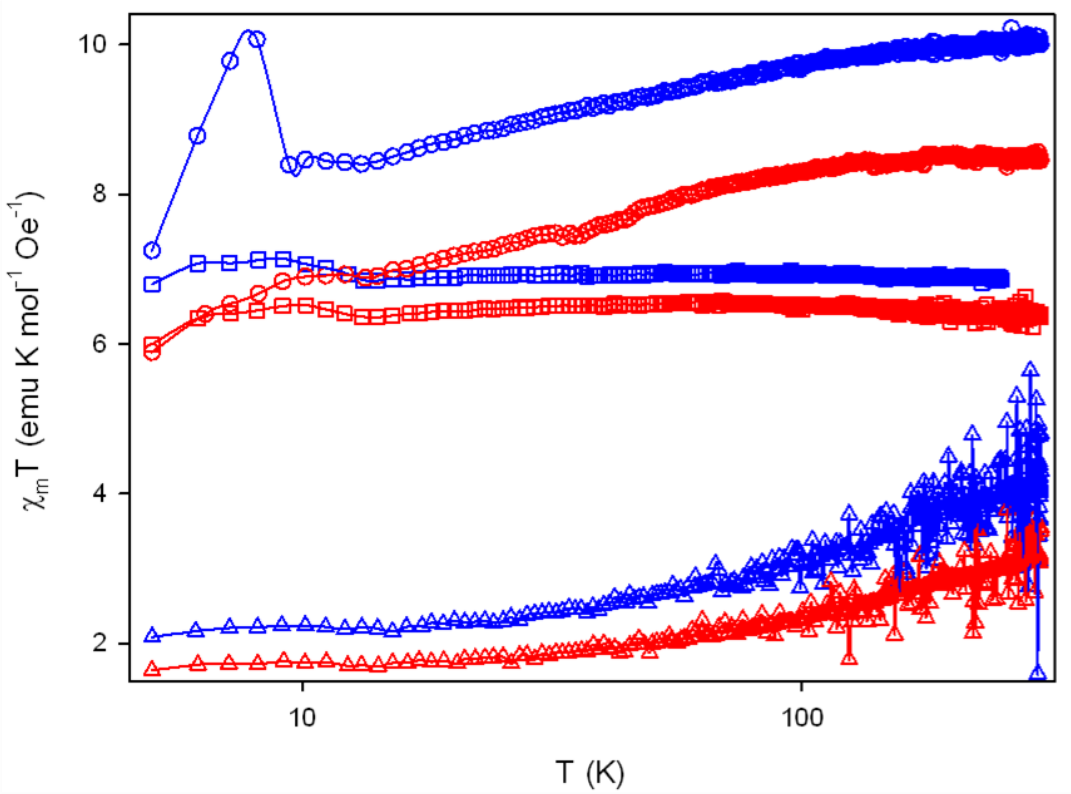

Figure 4: Magnetic susceptibility $\chi_m T$ as a function of temperature. DTAH (○), C_{10}mimH (○), DTAG (□), C_{10}mimG (□), DTAC (x 10, Δ), C_{10}mimC (x 10, Δ).

The magnetic behaviour of the Ce compounds was slightly different. A plot of $1/\chi_m$ vs T (Figure S5) suggests a phase transition at 12.2 K (T_N); understood to be from antiferromagnetism to paramagnetism and similar to literature values for crystalline β-Ce.[20] The likelihood is that Ce compounds are antiferromagnetic at lower temperature and paramagnetic at higher temperatures.

Compound	M_w / (g mol^{-1})	cmc / mM	β	$\chi_m T$/ (emu K mol^{-1} Oe^{-1})	μ_{eff} / μ_B	θ_{cw} / K	T_c / K	T_N / K
DTAB	308.35	15.5	0.26	-	-	-	-	-
DTAH	579.34	11.6	0.76	10.15	9.05 (10.6$^{\#}$)	4.09	5.1	-
DTAG	571.66	11.9	0.59	6.89	7.45* (7.94$^{\#}$)	0.06	-	-
DTAC	554.53	10.9	0.82	0.43	1.86 (2.54$^{\#}$)	-60	-	12.2
C_{10}mimCl	258.61	37.0	0.55	-	-	-	-	-
C_{10}mimH	529.89	31.3	0.74	8.55	8.41 (10.6$^{\#}$)	2.78	-	-
C_{10}mimG	522.21	30.0	0.82	6.41	7.19 (7.94$^{\#}$)	-0.18	-	-
C_{10}mimC	505.08	27.6	0.75	0.32	1.61 (2.54$^{\#}$)	-72	-	12.2

Table 2: Selected physical properties of surfactants. *At 250 K. $^{\#}$Calculated moment.

Surface Tensiometry in a Magnetic Field

Pendant drop measurements were made to determine the effect of magnetic field on surfactant solutions (Figure 5). In the absence of an applied field, the magnetic surfactants behave like conventional inert surfactants and lower the surface tension (γ) at the air-water interface. In fact, they are more efficient surfactants than their parent surfactant, showing greater γ reduction of water for the same concentration (Figure 5). On placing a magnet (0.4 T) in close proximity (~1 mm) to aqueous solutions of the Gd and Ho based surfactants γ reduces even further. The magnetic surfactants may therefore be considered bi-functional, being both intrinsically surface active and also showing a magnetically induced reduction in γ (possibly due to unpaired electrons aligning with the external field and anion partitioning at the interface). The effect is often quite remarkable: for example, γ of C_{10}mim H solutions reduces by a further 12 % in the applied magnetic field.

It is important to note that for the inert surfactants γ increased by about 1 mN m^{-1} in the magnetic field. This is perhaps not so unusual, as recent reports[21] have shown that strong magnets can indeed affect γ for liquid water, believed to be due to development of hydrogen-bonding and a weakening of van der Waals forces. In fact it actually implies that the real magnetic surface reduction is around 1 mN m^{-1} greater than observed for Gd and Ho based surfactants and explains the slight increase observed for the Ce based surfactants.

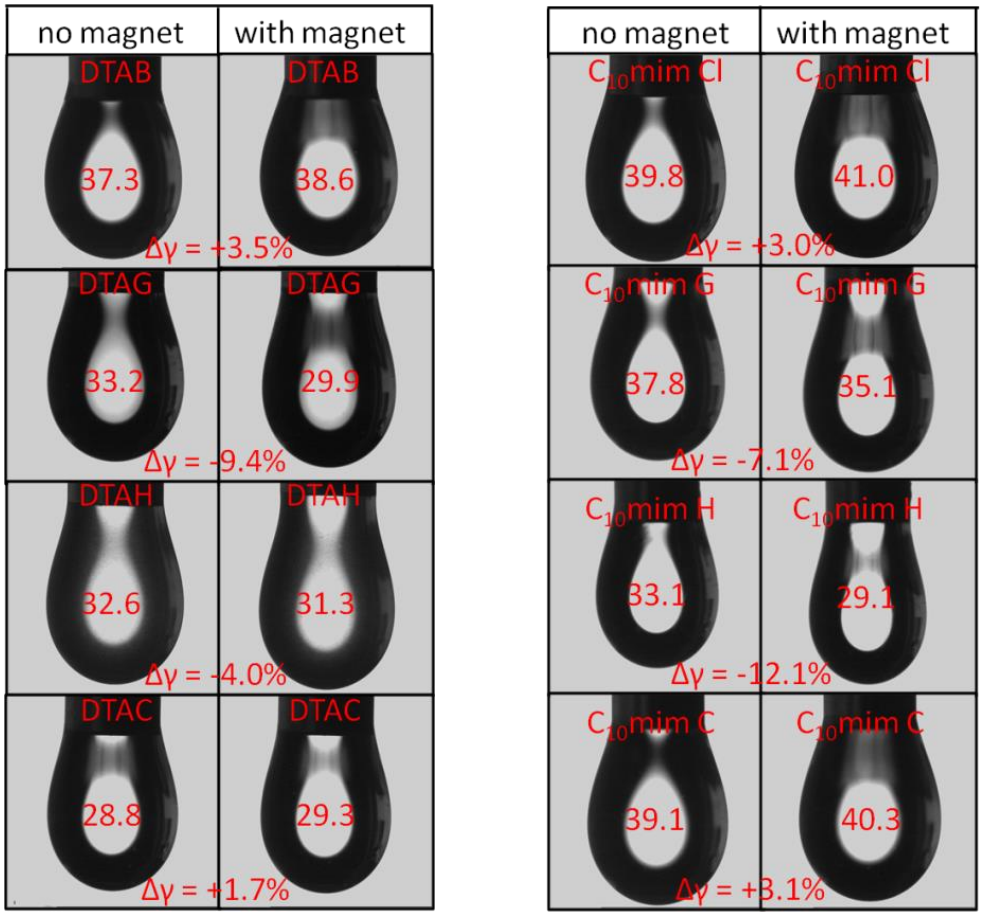

Figure 5: Pendant drop profiles of magnetic surfactants (0.10 M) with and without a magnet.

Units of surface tension γ are mN m^{-1}.

Effects of Micellar Structure on Magnetic Behaviour

It has recently been demonstrated that the formation of microemulsions by magnetic anionic surfactants leads to a large increase in magnetic susceptibility (as compared to solid surfactant samples) and a change in magnetic behaviour (paramagnetic in the solid to superparamagnetic in solution) attributed to a loss of bulk anisotropy, when surfactant molecules are partitioned at the oil/water interface.[9] In addition, the first magnetic surfactants to be reported were all based on hydrophobic $FeCl_4^-$ counterions.[1] It was suggested that these anions could reside in the micellar core. However, in this study there was no detailed investigation on the magnetic properties of the micellar solutions. It is therefore of interest to ascertain how the formation and structuring of micelles might affect magnetic susceptibility and phase behaviour of the surfactants studied here. In order to test this, the effective magnetic moment of the solution was determined (by VSM) as a

function of concentration for C_{10}mimH (Figure 6). This is similar to conductivity *vs.* concentration plots where a change in gradient may be observed at the cmc.[12a] The expected cmc was recorded by electrical conductivity at 31.3 mM (Table 2, Figure 6) and corroborated by SANS ((31 +1.5/-1.0) mM), Figure S6).

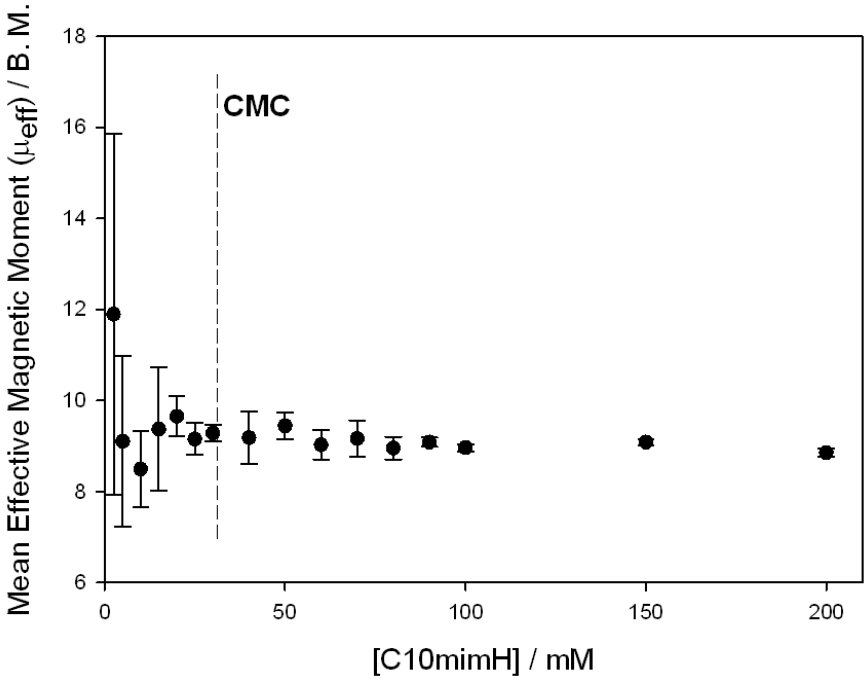

Figure 6: The relationship between the mean effective magnetic moment μ_{eff} and the concentration of the C_{10}mimH.

The corrected magnetization graphs for all concentrations show straight lines with no sign of hysteresis (Figure S7). The measured value for the volume susceptibility of water, χ_{H2O}, is (-6.78 ± 1.36)·10^{-6} and differs from the literature value of (-9.04·10^{-6}) by 25 %.[22] The relative standard deviation increases with decreasing concentration of C_{10}mimH below 20 mM, up to 33.4 % for sample for the concentration of 2.5 mM, and no trend can be observed in the plot (Figure 6) with the mean value for the effective magnetic moment of 9.30 ± 0.73 μ_B. The most probable reason that no transition was observable is that the magnetic counterions in these systems are highly dissociated (Table 2) with as few as ~20 % of the magnetic counterions "structured" around the micelles. This is in complete contrast to the microemulsions (inverse micelles) recently studied[9],

where, although dissociated, the counterions are partitioned into the small volume of the aqueous droplet and are in close proximity.

Conclusions

This paper introduces new magnetic surfactants that have greater magnetic responsivity than previously reported systems.[1] The liquid crystalline and magnetic phase behaviour of these new surfactants indicate they may be considered as novel molecular magnets,[8] with interspin coupling tunable through manipulation of molecular architecture, selection of metal ion and now potentially aggregation. For the cationic surfactant systems studied here at room temperature, aggregation (micellization) appears to have no noticeable effects on molar magnetic susceptibility: it was not possible to determine a critical micelle concentration by magnetometry. However, a wider range of magneto-surfactants would need to be studied to confirm this behaviour more generally. This study does reveal that even very dilute systems exhibit magnetic susceptibility, which should be controllable given a large enough applied magnetic field. Finally, magnetic effects on surface tension combined with catalytic and luminescent properties of lanthanide metals suggest diverse and interesting potential applications.[4, 7]

Acknowledgements

PB thanks HEFCE and University Bristol, School of Chemistry for a DTA, PhD scholarship. We acknowledge the Krüss Surface Science Centre, Bristol, for surface tension facilities, and the Science and Technology Facilities Council for the allocation of beam time, travel, and consumables grants at ILL and ISIS. For financing, the DFG (Emmy Noether programme, A. S.) is acknowledged. We also thank Prof. Walther Schwarzacher of the Surface Physics group (Bristol University) for the use of the SQUID magnetometer.

Supporting Information

SANS Scattering Laws and Model Fitting

Scattering intensity *I(Q)* is linked to the size and shape of the aggregates (form factor, *P(Q)*) and the interaction between these aggregates (structure factor, S(Q)),

$$I(Q) \propto P(Q,R)S(Q) \qquad \text{Eq. S1}$$

where *R* is the particle radius.

Different models were employed to fit the raw data using the FISH[23] interactive fitting program, which can be found online (http://www.small-angle.ac.uk). DTAB and C_{10}mimCl used the model for an ellipsoid form factor (*P*(*Q*)) multiplied by a Hayter-Penfold charge repulsion (*S*(*Q*)), giving the effective structure factor for charged micelles.[24]

There are two structural dimensions in the ellipsoidal form factor model used, and these are the radius of the principal axis, R_1, with *X* the axial ratio. *X* is 1 for a spherical, < 1 for an oblate and > 1 for a prolate structure. Fit parameters in the model were: ellipsoid *P*(*Q*), principal radius R_1, aspect ratio *X*; *S*(*Q*), micellar charge *Z*, volume fraction, ϕ, Debye length, κ^{-1}, and the effective radius of the charged micelle, $R_{S(Q)}$.

For *S*(*Q*) the value of ϕ is known based on composition and κ can be estimated to a first approximation using

$$\kappa = \left(\frac{2\mathrm{F}^2\rho I}{\varepsilon_0 \varepsilon_r \mathrm{R}T}\right) \qquad \text{Eq. S2}$$

where F is the Faraday constant, ρ is the solvent density, *I* the ionic strength, ε_0 is the permittivity of free space and ε_r is the dielectric constant of the solvent. κ^{-1} has the dimensions of length and is a measure of the extent of the electric double layer.

All other surfactants were fitted using a hard sphere structure factor (*HSS(Q)*),[25] fitting to parameters of R_1, *X*, and hard sphere volume fraction, HSϕ.

SQUID Magnetometry of Solid Samples

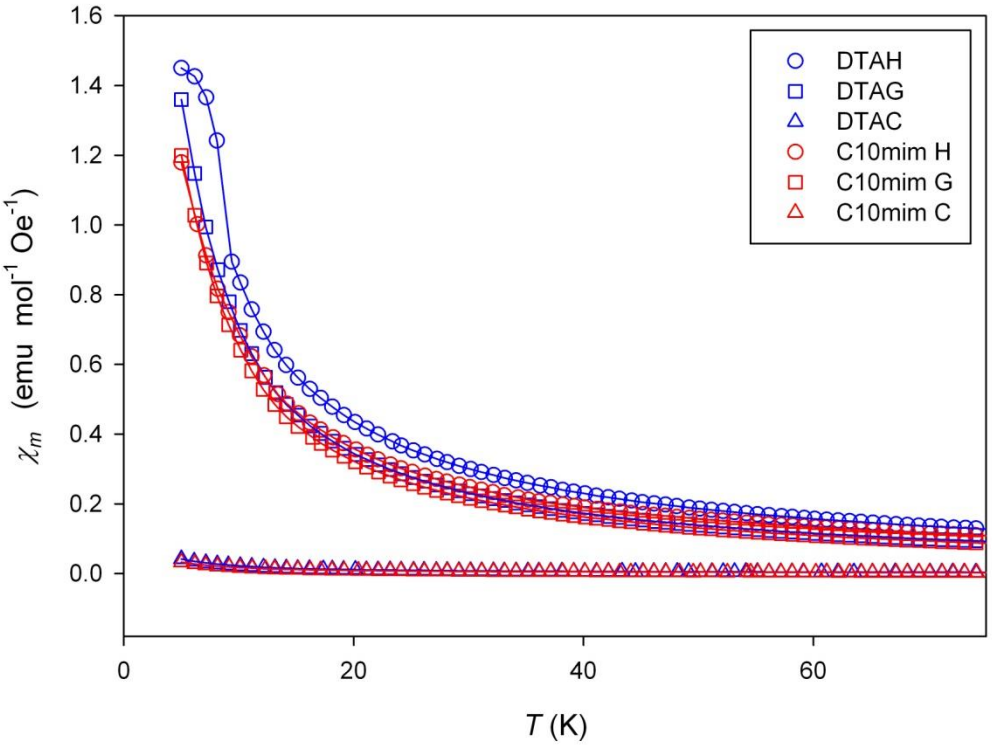

Figure S1: SQUID magnetometry data showing molar magnetic susceptibility χ_m as a function of temperature *T*.

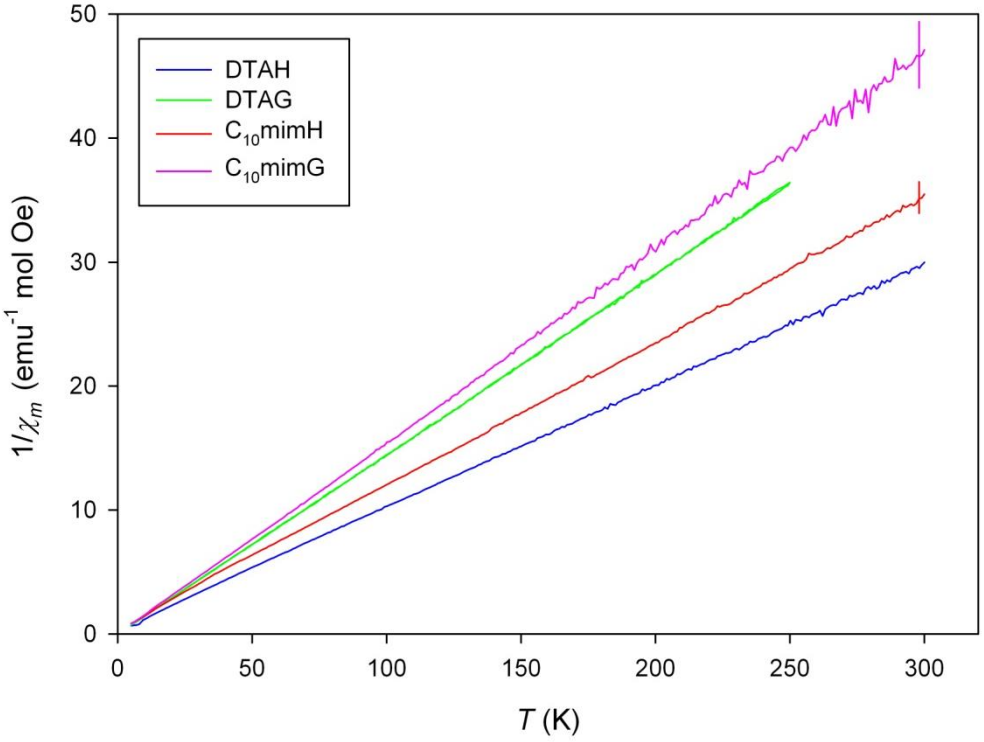

Figure S2: SQUID magnetometry data showing temperature dependence of $1/\chi_m$ for the paramagnetic surfactants measured under 0.50 kOe.

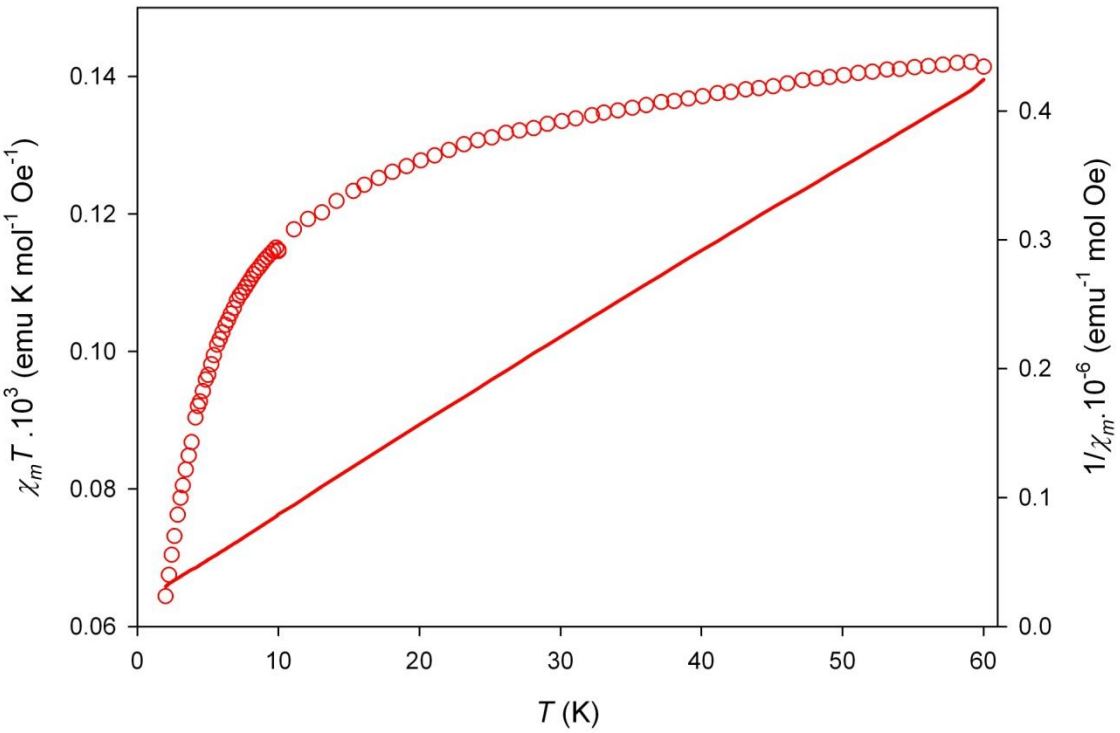

Figure S3: SQUID magnetometry data showing temperature dependence of $\chi_m T$ (red circles) and $1/\chi_m$ (red line) for C_{10}mimH.

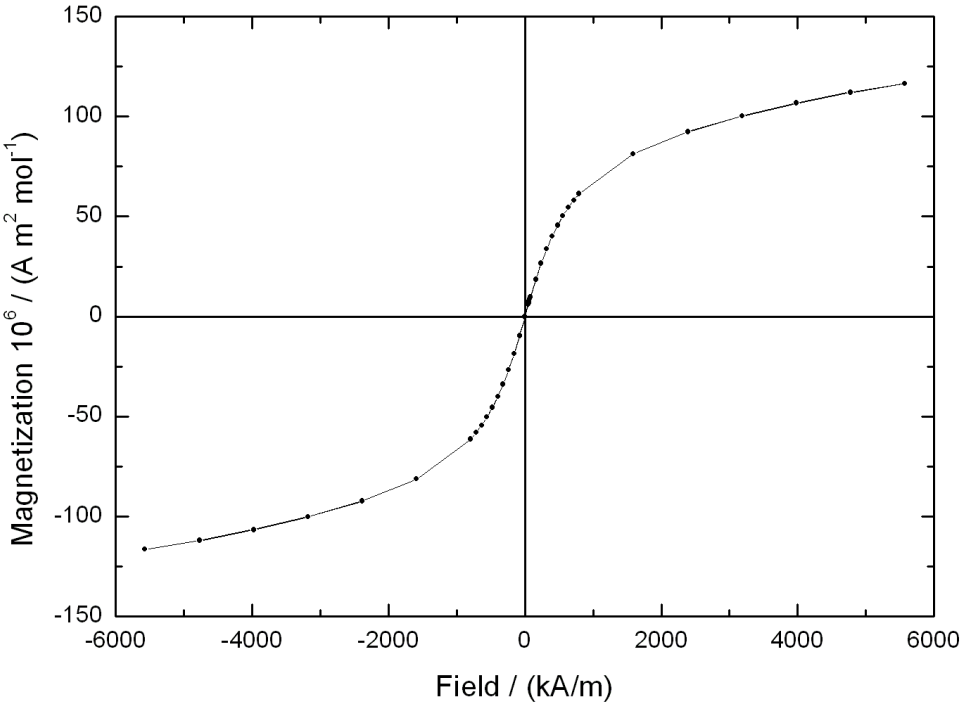

Figure S4: SQUID magnetometry data showing full hysteresis slope for C_{10}mimH at 2K.

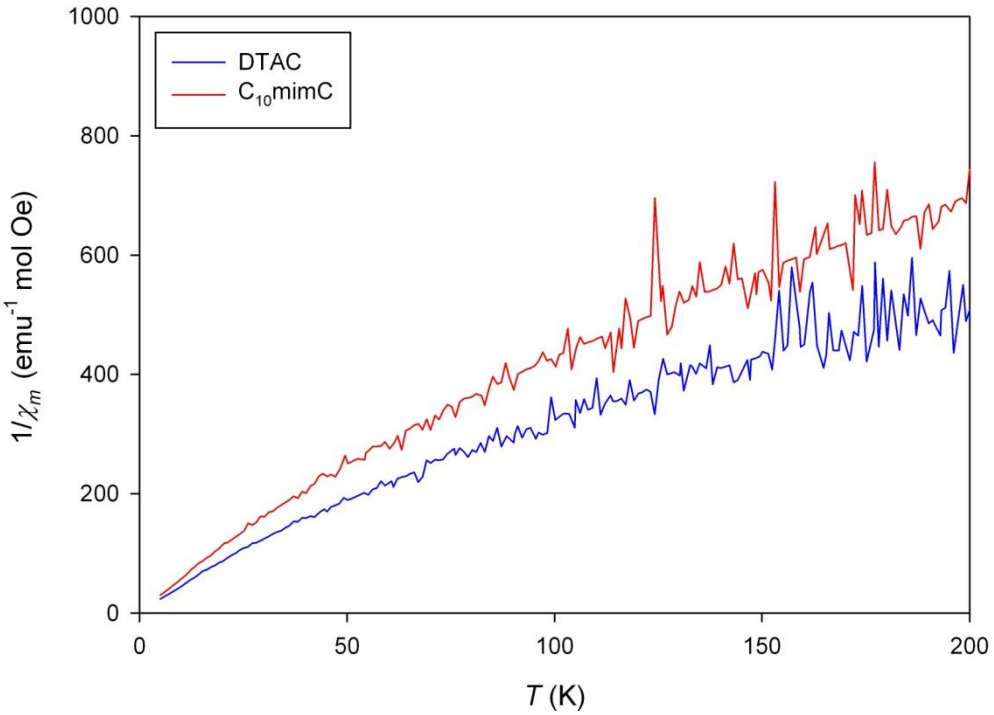

Figure S5: SQUID magnetometry data showing temperature dependence of $1/\chi_m$ for cerium-based surfactants measured under 0.50 kOe.

Effects of Micellar Structure on Magnetic Behaviour Investigated Using Vibrating Sample Magnetometry

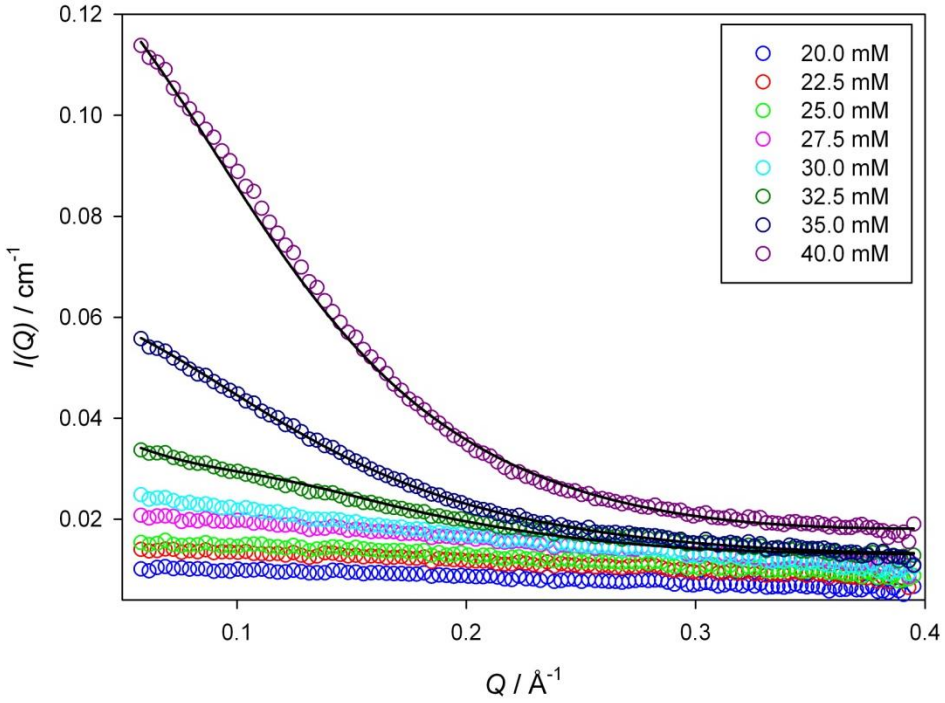

Figure S6: SANS profiles for C10mimH as a function of concentration. Lines indicate fitted profiles for surfactants above the cmc.

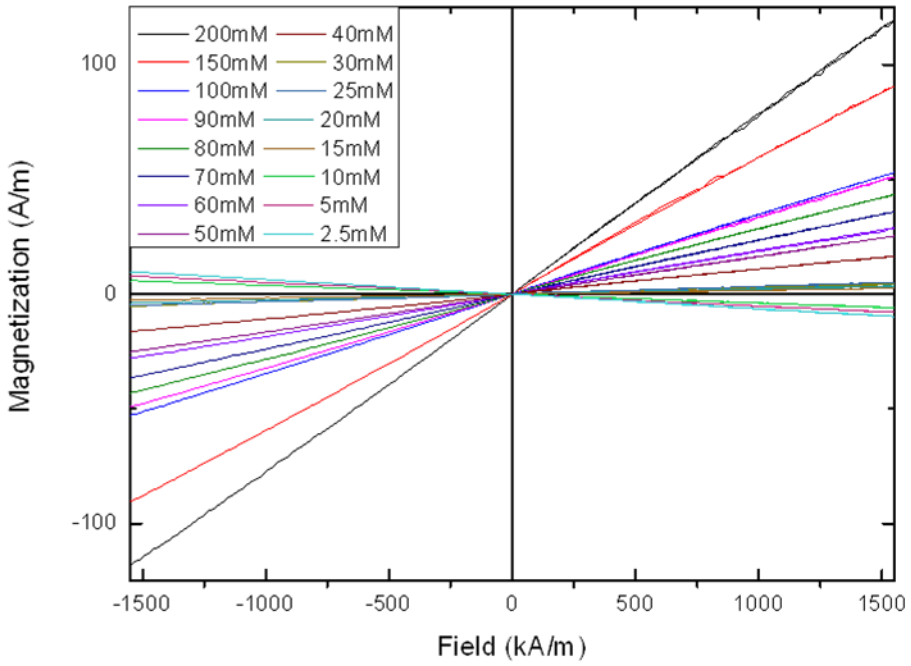

Figure S7: VSM curves of the solutions made from C10mim Ho with different concentrations (1st series of measurements).

***C* [mM]**	μ_{eff} / μB	$\Delta\mu_{eff}$ / μB	$\Delta\mu_{eff}$ / %
200	8.86	0.09	1.04
150	9.09	0.07	0.75
100	8.97	0.08	0.84
90	9.09	0.10	1.12
80	8.96	0.25	2.78
70	9.17	0.40	4.41
60	9.03	0.32	3.52
50	9.45	0.29	3.04
40	9.19	0.57	6.21
30	9.29	0.18	1.98
25	9.16	0.35	3.77
20	9.66	0.44	4.52
15	9.38	1.36	14.5
10	8.50	0.84	9.83
5	9.11	1.87	20,6
2.5	11.9	3.96	33.4

Table S1: Calculated mean values for the effective magnetic moment μ_{eff} and standard deviation $\Delta\mu_{eff}$.

References

1. Brown, P.; Bushmelev, A.; Butts, C. P.; Cheng, J.; Eastoe, J.; Grillo, I.; Heenan, R. K.; Schmidt, A. M., *Angewandte Chemie International Edition,* 2012, 2414.
2. Brown, P.; Butts, C. P.; Cheng, J.; Eastoe, J.; Russell, C. A.; Smith, G. N., *Soft Matter* 2012, 8, 3545.
3. Brown, P.; Khan, A. M.; Armstrong, J. P. K.; Perriman, A. W.; Butts, C. P.; Eastoe, J., 2012, 24, 6244.
4. Marciniec, B., *Hydrosilylation: A Comprehensive Review on Recent Advances*. Springer: New York, 2009.
5. Pfleiderer, C., *Reviews of Modern Physics,* 2009, *81*, 1551.
6. Solomon, S., *Ceramics International,* 2012, *38*, 599.
7. Beeby, A.; Clarkson, I. M.; Eastoe, J.; Faulkner, S.; Warne, B., *Langmuir,* 1997, *13*, 5816.
8. Blundell, S. J.; Pratt, F. L., *Journal of Physics: Condensed Matter ,* 2004, *16*, R771.
9. Brown, P.; Butts, C. P.; Eastoe, J.; Glatzel, S.; Grillo, I.; Hall, S. H.; Rogers, S.; Trickett, K., *Soft Matter ,* 2012, 8, 11609.
10. Del Sesto, R. E.; McCleskey, T. M.; Burrell, A. K.; Baker, G. A.; Thompson, J. D.; Scott, B. L.; Wilkes, J. S.; Williams, P., *Chemical Communications,* 2008, 447.
11. Brown, P.; Butts, C.; Dyer, R.; Eastoe, J.; Grillo, I.; Guittard, F.; Rogers, S.; Heenan, R., *Langmuir,* 2011, 27, 4563.
12. (a) Rodríguez, J. R.; González-Pérez, A.; Del Castillo, J. L.; Czapkiewicz, J., *Journal of Colloid and Interface Science,* 2002, *250*, 438; (b) Cummings, S.; Enick, R.; Rogers, S.; Heenan, R.; Eastoe, J., *Biochimie,* 2012, *94*, 94.
13. Kwok, D. Y.; Neumann, A. W., *Advances in Colloid and Interface Science,* 1999, *81*, 167.
14. Pallas, N. R.; Harrison, Y., *Colloids and Surfaces,* 1990, *43*, 169.
15. McGrath, K. M., *Langmuir ,*1995, *11*, 1835.
16. Griffiths, P. C.; Paul, A.; Khayat, Z.; Heenan, R. K.; Ranganathan, R.; Grillo, I., *Soft Matter,* 2005, *1*, 152.
17. Goodchild, I.; Collier, L.; Millar, S. L.; Prokes, I.; Lord, J. C. D.; Butts, C. P.; Bowers, J.; Webster, J. R. P.; Heenan, R. K., *Journal of Colloid and Interface Science,* 2007, *307*, 455.
18. Strandburg, D. L.; Legvold, S.; Spedding, F. H., *Physical Review,* 1962, *127*, 2046.
19. *Handbook of Magnetic Materials*. Elsevier: Amsterdam, 2012.
20. Burgardt, P.; Gschneidner, K. A., Jr.; Koskenmaki, D. C.; Finnemore, D. K.; Moorman, J. O.; Legvold, S.; Stassis, C.; Vyrostek, T. A., *Physical Review B,* 1976, *14*, 2995.

21. (a) Cai, R.; Yang, H.; He, J.; Zhu, W., *Journal of Molecular Structure,* 2009, *938*, 15; (b) Holysz, L.; Szczes, A.; Chibowski, E., *Journal of Colloid and Interface Science,* 2007, *316*, 996.

22. Arrighini, G. P.; Maestro, M.; Moccia, R., *The Journal of Chemical Physics ,* 1968, *49*, 882.

23. Heenan, R. K. *Fish Data Analysis Program*; Rutherford Appleton Laboratory pp RAL, 1989.

24. (a) Hayter, J. B.; Penfold, J., *Molecular Physics,* 1981, *42*, 109; (b) Hansen, J. P.; Hayter, J. B., *Molecular Physics,* 1982, *46*, 651; (c) Hayter, J. B.; Penfold, J., *Colloid and Polymer Science,* 1983, *261*, 1022.

25. Ashcroft, N. W.; Lekner, J., *Physics Review,* 1966, *145*, 83.